The American Journal of Pathology, Vol. 187, No. 2, February 2017

ELSEVIER

The American Journal of
PATHOLOGY
ajp.amjpathol.org

BIOMARKERS, GENOMICS, PROTEOMICS, AND GENE REGULATION

Neuronal Protein 3.1 Deficiency Leads to Reduced Cutaneous Scar Collagen Deposition and Tensile Strength due to Impaired Transforming Growth Factor-β1 to -β3 Translation

Tao Cheng,* Michael Yue,* Muhammad Nadeem Aslam,† Xin Wang,‡ Gajendra Shekhawat,‡ James Varani,† and Lucia Schuger*

From the Department of Pathology, The University of Chicago Medical School, Chicago, Illinois; the Department of Pathology,† The University of Michigan Medical School, Ann Arbor, Michigan; and the Department of Materials Science and Engineering,‡ Northwestern University, Evanston, Illinois*

Accepted for publication October 6, 2016.

Address correspondence to Lucia Schuger, M.D., Department of Pathology, The University of Chicago Medical School, 5841 S. Maryland Ave., Chicago, IL 60637. E-mail: lschuger@bsd.uchicago.edu.

Neuronal protein 3.1 (P311), a conserved RNA-binding protein, represents the first documented protein known to stimulate transforming growth factor (TGF)-β1 to -β3 translation *in vitro* and *in vivo*. Because TGF-βs play critical roles in fibrogenesis, we initiated efforts to define the role of P311 in skin scar formation. Here, we show that P311 is up-regulated in skin wounds and in normal and hypertrophic scars. Genetic ablation of *p311* resulted in a significant decrease in skin scar collagen deposition. Lentiviral transfer of P311 corrected the deficits, whereas down-regulation of P311 levels by lentiviral RNA interference reproduced the deficits seen in $P311^{-/-}$ mice. The decrease in collagen deposition resulted in scars with reduced stiffness but also reduced scar tensile strength. *In vitro* studies using murine and human dermal fibroblasts showed that P311 stimulated TGF-β1 to -β3 translation, a process that involved eukaryotic translation initiation factor 3 subunit b as a P311 binding partner. This resulted in increased TGF-β levels/activity and increased collagen production. In addition, P311 induced dermal fibroblast activation and proliferation. Finally, exogenous TGF-β1 to -β3, each restituted the normal scar phenotype. These studies demonstrate that P311 is required for the production of normal cutaneous scars and place P311 immediately up-stream of TGF-βs in the process of fibrogenesis. Conditions that decrease P311 levels could result in less tensile scars, which could potentially lead to higher incidence of dehiscence after surgery. *(Am J Pathol 2017, 187: 292—303; http://dx.doi.org/10.1016/j.ajpath.2016.10.004)*

Neuronal protein 3.1 (P311) is a conserved 8-kDa protein[1] expressed in vascular and visceral smooth muscle beds,[2] the nervous system,[2,3] regenerating tissues,[4–7] and malignant glioblastomas.[8] P311 has been shown to induce myofibroblast differentiation and migration[4,9] and to promote nerve and lung regeneration.[5,6] Deletion of *p311* in mice was reported originally to result in no overt phenotype,[10] although these animals displayed learning and memory defects.[10,11] More recently, however, we reported that genetic ablation of P311 leads to decreased vascular smooth muscle cell contractility, hypotonic blood vessels, and vascular hypotension due to a defect in transforming growth factor (TGF)-β1 to -β3 translation.[2] Basic Local Alignment Search Tool (BLAST) searching reveals that P311 does not belong to any known protein family and has no established functional motif that might indicate function. Therefore, the molecular mechanisms of P311 biological action have remained unknown for years, until recently when we found that P311 is an intrinsically disordered protein requiring, therefore, an interacting partner to acquire tertiary structure and function.[1] We identified eukaryotic translation initiation factor 3 subunit b (eIF3b) as a P311 binding partner.[1] Their binding sites were mapped to the noncanonical RNA recognition motif of eIF3b and a central 11 amino acid-long region of P311 that we referred to as eIF3b binding motif.

Supported by NIH grant R01GM111116 (L.S. and J.V.).
Disclosures: None declared.

http://dx.doi.org/10.1016/j.ajpath.2016.10.004

As part of our characterization, we demonstrated that P311 directly binds to TGF-β1 to -β3 5′ untranslated regions of mRNAs through a previously unrecognized RNA recognition motif-like motif, identifying P311 as an RNA binding protein.[1] Then we went on to showing that, by concomitantly binding to translation initiation factor eIF3b and to the 5′ untranslated region of TGF- β1 to -β3 mRNAs, P311 recruits TGF-β1 to -β3 mRNAs to the translation machinery, which in turn leads to increased translation of TGF-βs and to the up-regulation of TGF-β1 to -β3 levels.[1] P311 is, therefore, the first documented regulator of all three TGF-βs and the only protein currently known to stimulate TGF-β translation *in vitro* and *in vivo*.

It has been long established that TGF-β1 plays a central role in the promotion of fibrogenesis.[12–17] The role of TGF-β2 in fibrogenesis has been far less studied, but a number of reports indicate that it also promotes fibrosis.[18–21] Unlike the previous two, the TGF-β3 participation in the process of fibrosis is less clear. Starting with Shah et al,[22] multiple studies showed that TGF-β3 has a protective effect against fibrosis,[23,24] a view that gained widespread support.[15,25] However, there are several reports indicating that, like the other two TGF-βs, TGF-β3 is also fibrogenic.[26–29] In support of this latter view, recombinant TGF-β3 (Avotermin) showed no antiscarring effect in clinical trials.[30]

Because P311 stimulates up-regulation of all three TGF-βs, we sought to determine whether P311 might play a functional role in fibrogenesis, focusing on cutaneous scar formation as a model. Scarring is the end point of adult cutaneous wound healing, which can be divided into the following three phases: inflammatory, proliferative, and remodeling. Scar formation takes place in the remodeling phase.[25] Wound healing is therefore an imperfect process that inevitably leads to scar formation as the skin re-establishes its integrity. Scar tissue has different characteristics compared with normal skin, ranging from fine-line asymptomatic scars to problematic scarring that includes hypertrophic and keloid scars. Scar tissue can differ in color to the surrounding skin. Scar tissue can be flat, stretched, depressed, or raised and can manifest a range of features, including inflammation, erythema, dryness, and pruritus. Together, these characteristics can have significant psychosocial impact on patients and their quality of life. Because of the significant impact that scarring can have in the quality of life, much research is still being devoted to understanding mechanisms of scar formation and to minimizing its impact. However, past and current antiscarring therapies have met limited success.[31]

We indeed found that P311 production is switched on in healing wounds and normal and hypertrophic scars compared with normal skin, in which it is absent, indicating a potential role for P311 in scar formation. Indeed, *in vivo* and *in vitro* studies indicated that, because of its stimulation of TGF-β1 to -β3 translation, P311 is required for collagen deposition and tensile strength during normal scar formation which, in turn, is essential to prevent scar dehiscence. Furthermore, these studies showed that all three TGF-βs are fibrogenic and placed P311 as a stimulator of fibrosis acting immediately upstream of TGF-β1 to -β3.

Materials and Methods

IHC

Four samples of normal skin and four samples of hypertrophic scars were obtained from the University of Chicago Pathology Core Facility. Immunohistochemistry (IHC) was performed at the University of Chicago Pathology Core Facility. Briefly, The IHC procedure was applied to formalin-fixed, paraffin-embedded 5-μm tissue sections, which were incubated with anti-human P311 antibody[2] (1:50 dilution) after antigen unmasking by boiling in fresh citrate buffer. The reactions were developed with Vectastain ABC kit (Vector Laboratories, Burlingame, CA).

Mice

Generation of $P311^{-/-}$ mice (C57BL/6 mice with deletion of the entire P311 coding region on both alleles) was previously described.[10] Four-month-old males were used in this study, and age-matched wild-type (WT) C57BL/6 mice (Charles River Laboratories, Wilmington, MA) were used as controls. Animals were housed at the University of Chicago animal facility (20°C approximately 25°C and 12-hour light cycle) and supplied with rodent diet no. 2918 (18% protein, 6% fat, and moderate phytoestrogen; Harlan Laboratories, Indianapolis, IN). All studies involving animals were reviewed and approved by the Institutional Committee on Use and Care of Animals.

Cell Culture

Primary mouse skin fibroblasts (MFs) (C57Bl/6), primary human foreskin fibroblasts (HFs), and primary human foreskin keratinocytes (HKs) were isolated as previously described[32] and cultured in Dulbecco's modified Eagle's medium (DMEM) containing 10% fetal bovine serum (HyClone Laboratories, Logan, UT), 2 mmol/L L-glutamine, and antibiotic-antimycotic reagent (Anti-Anti; Gibco, Grand Island, NY). For all experiments, cells were incubated at 37°C in an atmosphere of 95% air and 5% CO_2. To generate P311-positive MFs and HFs, cells at approximately 70% confluence were transfected with the P311 expression construct pCMV-Myc-P311 (Clontech, Palo Alto, CA) using Lipofectamine 2000 reagent in Opti-MEM (Invitrogen, Carlsbad, CA). Cells transfected with vector alone were used as P311-negative counterparts. Twenty-four hours after transfection, the cells were used for biochemical and functional studies. For TGF-β determination, cells were washed twice with phosphate-buffered saline (PBS) and cultured in DMEM containing 10% charcoal-stripped fetal bovine serum (HyClone Laboratories) for 24 hours.

Excisional Wound Model

Mice were anesthetized with an intraperitoneal injection of ketamine/xylazine (100/10 mg/kg). An area of skin in the upper back was shaved, washed, and scrubbed with 75% alcohol to achieve aseptic conditions. Subsequently, 50 μL of 2% bupivacaine was locally injected to fully ensure pain elimination. A single 6-mm full-thickness punch biopsy was performed on each animal. Mice were photographed postoperatively at 0, 3, 7, 14, and 21 days using a Canon (Tokyo, Japan) high-resolution digital camera. The time of wound closure was recorded, and the scar area was determined on day 21. The mice were sacrificed to harvest normal skin, healing wound (day 14 after wounding), and scar (day 21 after wounding) for further studies.

Measurement of Scar Thickness

Resected scar tissue was formalin-fixed, paraffin-embedded and cut perpendicularly to the surface to generate 5-μm–thick sections from the center of the scar. The sections were mounted on glass slides and stained with hematoxylin-eosin. The maximal scar thickness was determined under a bright-field microscope with the aid of a micrometer-bearing lens piece.

Quantification of Scar Collagen by SHG Imaging

Histologic sections were stained with Picro Sirius for collagen quantification using second-harmonic generation (SHG) imaging. The SHG images were acquired with a Leica SP5 Tandem Scanner Spectral 2-Photon Confocal microscope (Leica Microsystems, Wetzler, Germany) and analyzed using ImageJ software version 1.50 (NIH, Bethesda, MD). Pixel counts in five different fields per slide were used to indicate the amount of collagen present.[33] The results were then expressed as the percentage of the total image area.

HYP Incorporation Assay

Ten-milligram samples from scar tissue and normal skin were homogenized in T-PER tissue protein extraction reagent (Pierce, Rockford, IL) after which 37% hydrochloric acid was added. The homogenates were mixed thoroughly and incubated at 120°C for 3 hours. The samples were then centrifuged at 15,000 × *g*. Ten microliters of supernatant fluid from each sample was transferred to a clear 96-well microplate. The content of the wells was evaporated overnight at 60°C. The hydroxyproline (HYP) content of each well was then determined using a HYP assay kit (MAK008; Sigma-Aldrich, St. Louis, MO). The absorbance at 560 nm was determined using a microplate reader (iMARK microplate reader; Bio-Rad, Hercules, CA). The absorbance value was converted to HYP content using a standard curve, and from this, collagen concentration was determined by multiplying by a factor of eight (based on the HYP content of collagen).[34]

P311 RNA Interference

Lentivirus vector carrying a P311 shRNA insert or scrambled control RNA (scRNA) were purchased from MISSION shRNA plasmid DNA (Sigma-Aldrich). 293T cells at approximately 70% confluence were transfected with the P311 shRNA plasmid or scRNA and package plasmids (pCMV-dR8.2 and pCMV-VSV-G); (Addgene, Cambridge, MA) using Lipofectamine 2000 reagent in Opti-MEM (Invitrogen). Forty-eight hours after transfection, lentivirus particles in the supernatant fluid were collected and purified using the Fast-Trap virus purification and concentration kit (Millipore, Billerica, MA), according to the manufacturer's protocol.

Excisional wounds were generated on the backs of $P311^{-/-}$ and WT mice as described. Twenty-four hours later, 1×10^8 lentivirus particles expressing the P311 shRNA or an equal amount of lentivirus expressing the scRNA control were dissolved in 30 μL of PBS and subcutaneously injected at the borders of the P311 WT wounds at four equidistant points. $P311^{-/-}$ mice, used for comparison, received PBS. After 21 days, the scars were removed for HYP-incorporation assays.

P311 Transfer

A lentivirus vector overexpressing P311 and the corresponding empty vector (EV) were purchased from DNASU Plasmid Repository (Biodesign Institute, Arizona State University). 293T cells at approximately 70% confluence were transfected with the P311-expressing plasmid or EV and package plasmids (pCMV-dR8.2 and pCMV-VSV-G; Addgene) using Lipofectamine 2000 reagent in Opti-MEM (Invitrogen). Forty-eight hours after transfection, the lentivirus particles in the supernatant fluid were collected and purified using the Fast-Trap virus purification and concentration kit (Millipore) according to the manufacturer's protocol.

Excisional wounds were generated on $P311^{-/-}$ and WT mice as described above. Twenty-four hours later, 1×10^8 lentivirus expressing P311 or equal amount of lentivirus control were suspended in 30 μL of PBS and subcutaneously injected at the borders of the $P311^{-/-}$ wounds at four equidistant points. WT mice, used for comparison, received PBS. After 21 days, the scars were removed for HYP assays.

Determination of Scar Stiffness

Skin wounds were generated on $P311^{-/-}$ and WT mice as described above, and scar tissue was collected on day 21. A 1-cm^2 piece of either normal skin or scar tissue was harvested and placed in ice-cold DMEM for immediate

elasticity measurements using atomic-force microscopy (AFM). An atomic-force microscope (Bruker ICON system; Bruker, Billerica, MA) bearing a silicon dioxide bead with a diameter of approximately 850 nm attached to a tipless silicon nitride triangular cantilever with 30-nm gold coating (Novascan Technologies, Ames, IA) was used. The deflection sensitivity was calibrated by repeated contact mode indentation on a clean glass slide (VWR International, Inc., Radnor, PA), and the spring constant of the compliant AFM cantilever was measured to be $\kappa = 0.19$ Nm-1 by the thermal noise method.[35] The tip radius was determined by scanning electron microscope (Hitachi SU8030; Hitachi, Yokohama, Japan). An optical microscopy image was taken during the AFM probe doing indentation on the target places. Elastic modulus was measured by fitting the experimental data to the spherical Hertzian contact mechanical model.[36] The MATLAB (MathWorks, Inc., Natick, MA) code was used to analyze the experimental data, where the goodness values R^2 exceeded 0.85 in all curve fittings as reported in Wang et al.[37] The measurements were repeated at more than six various positions with >10 measurements at each position on one sample.

Determination of Scar Tensile Strength

Mice were anesthetized as described above and dorsally shaved. Under aseptic surgical conditions, a dorsal midline incision extending from the scapulae to the base of the tail was created with a scalpel and closed with clips, which were removed 7 days later. The mice were sacrificed on day 21 after wounding, and a segment of the scar with surrounding normal skin at each side was removed and used for mechanical testing. A piece of normal skin of equal size served as control. The tissue specimens were attached to custom grips with double-sided tape for tensile strength measurements using a micro tester (Model ESM; MARK-10, Copiague, NY) by stretching at 5 mm/minute until rupture.[38]

Real-Time Quantitative PCR

Normal skin, healing wounds, scars, MFs, HFs, and HKs were used for RNA isolation and cDNA synthesis using the AURUMTM total RNA kit (Bio-Rad) and the iScript cDNA synthesis kit (Bio-Rad). Real-time PCR for cDNA was conducted using iQ SYBR Green Supermix (Bio-Rad) and the following primers for mouse: P311 sense, 5′-GCTACCAAGAGTGTGAGAGG-3′, and antisense, 5′-CTTTGGGAAAGGGATAATTT-3′; TGF-β1 sense, 5′-TGAGTGGCTGTCTTTTGACG-3′, and antisense, 5′-TTCTCTGTGGAGCTGAAGCA-3′; TGF-β2 sense, 5′-GTGACATGGACAGTGGATGC-3′, and antisense, 5′-GCGGACGATTCTGAAGTAGG-3′; TGF-β3 sense, 5′-TGGAGTCATGGCTGTAACT-3′, and antisense, 5′-CACTCACACTGGCAAGTAGT-3′; Collagen1A1 (COL1A1) sense, 5′-GGAAGAGCGGAGAGTACTGG-3′, and antisense, 5′-GGCTGAGTAGGGAACACACA-3′; Collagen3A1 (COL3A1) sense, 5′-CCTGGAGAGAAAGGTGAAGG-3′, and antisense, 5′-GTACCAGGACCACCAGGACT-3′; and glyceraldehyde-3-phosphate dehydrogenase sense, 5′-ATCACCATCTTCCAGGAGCGA-3′, and antisense, 5′-GCCAGT-GAGCTTCCCGTTCA-3′.

The following primers were used for human: P311 sense, 5′-TCCAAACAAGGACATGGAGGG-3′, and antisense, 5′-AGGTAACTGATTCTTGGGGAG-3′; TGF-β1 sense, 5′-GCCTTTCCTGCTTCTCATGG-3′, and antisense, 5′-TCCTTGCGGAAGTCAATGTAC-3′; TGF-β2 sense, 5′-CCCCACATCTCCTGCTAATG-3′, and antisense, 5′-ATGTAAAGTGGACGTAGGCAG-3′; TGF-β3 sense, 5′-AGTGGCTGTCCTTTGATGTC-3′, and antisense, 5′-CACCTCGTGAATGTTTTCCAG-3′; COL1A1 sense, 5′-CCCCTGGAAAGAATGGAGATG-3′, and antisense, 5′-TCCAAACCACTGAAACCTCTG-3′; COL3A1 sense, 5′-AAGTCAAGGAGAAAGTGGTCG-3′, and antisense, 5′-CTCGTTCTCCATTCTTACCAGG-3′; GAPGH sense, 5′-ATGCCTCCTGCACCACCAAC-3′, and antisense, 5′-GGCAGTGATGGCATGGACTG-3′.

TGF-β ELISA

Acidified lysates from normal skin, healing wounds, and scar tissue, as well as acidified MF, HF, and HK supernatant fluids were used for assessment of each of the three TGF-βs (TGF-β1 to -β3). The assays were performed with the DuoSet ELISA (enzyme-linked immunosorbent assay) kit (R&D Systems, Minneapolis MN) according to the manufacturer's instructions.

Western Blot Analysis

Normal skin, healing wounds, scar tissue, MFs, HFs, and HKs were lysed in RIPA lysis buffer (Sigma-Aldrich) containing proteinase inhibitors (Roche, Indianapolis, IN) and kept at 4°C for 20 minutes with rotation. Lysates were cleared by centrifugation for 10 minutes at 12,000 × rpm, and supernatant fluids were collected. Immunoblots were performed as previously described.[2] The following antibodies were used: anti-P311,[2] anti-pSMAD2, and anti-SMAD2 (both from Cell Signaling Technology, Danvers, MA), anti-pSMAD3 and anti-SMAD3 (both from R&D Systems.), anti-COL1A1 and anti-COL3A1 (both from Abcam, Cambridge, MA). Anti−glyceraldehyde-3-phosphate dehydrogenase (Santa Cruz Biotechnology, Santa Cruz, CA) was used as a loading control. The antibodies were used at the dilutions recommended by the manufacturers.

Luciferase Reporter Assay

TGF-β1 to -β3 5′ and 3′ untranslated regions were cloned into the pGL3-promoter firefly luciferase vector (Promega, Madison, WI) to generate reporter constructs.[1] MFs or HFs were plated in 6-well plates and transfected with a P311 expression vector or EV control, eIF3b siRNA or scRNA, all

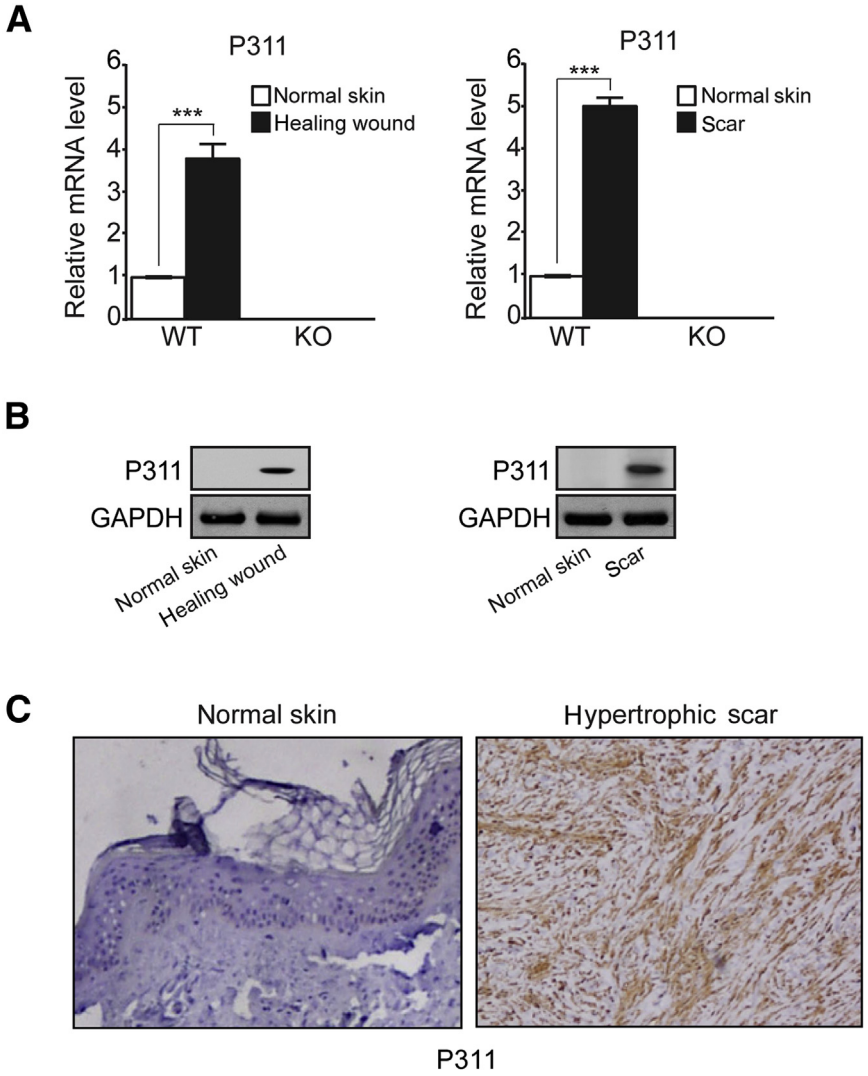

Figure 1 P311 expression is up-regulated in skin wounds and in normal and hypertrophic scars. **A:** qPCR showing expression of P311 mRNA in normal skin, healing wound (day 14 after wound), and scar (day 21 after wound) in WT and P311$^{-/-}$ mice. **B:** Representative Western blot analyses showing P311 in normal skin, healing wound (day 14 after wound), and scar (day 21 after wound) in WT mice. **C:** Representative IHC stains for P311 in human normal skin and dermis of human hypertrophic scars; positivity is represented by brown color. Data are expressed as means ± SD. $n = 5$ mice per group (**A** and **B**); $n = 4$ mice per group (**C**). $***P < 0.001$. Original magnification, ×20. GAPDH, glyceraldehyde-3-phosphate dehydrogenase; IHC, immunohistochemistry; KO, knockout; P311, neuronal protein 3.1; qPCR, real-time quantitative PCR; WT, wild-type.

described in Yue et al,[1] the reporter constructs, and Renilla luciferase internal control vector pRL-SV40. Forty-eight hours after cotransfection, the Dual-Luciferase reporter assay system (Promega) was used to determine the ratio of firefly to Renilla luciferase activity, as indicated by the manufacturer.

Cell Proliferation Assay

MFs or HFs (3×10^3 cells) transfected with P311 or EV control were seeded in complete medium in a 96-well plate and cultured for 0 hour, 24, 48, or 72 hours. Then 10 μL of bromodeoxyuridine solution from bromodeoxyuridine proliferation assay kit (Calbiochem, San Diego, CA) was added and incubated for 2 hours. The cells were then fixed according to the manufacturer's instructions, and absorbance was measured at 450 nm.

Cell Migration Assay

Modified Boyden chambers with 8-μm pore polycarbonate membranes (Corning, Corning, NY) fitted for 24-well plates were used for this assay. MFs or HFs (1×10^5 cells) transfected with P311 or with EV control were suspended in 100 μL of serum-free culture medium and seeded in the upper compartment of the migration chambers. Complete medium was added in the lower compartment. The cells were allowed to migrate for 8 hours at 37°C in 95% air and 5% CO_2. At the end of this period, the upper surface of the membrane was wiped with a cotton swab to remove nonmigratory cells. Cells that had migrated through the pores to the lower side of the membrane were fixed with 4% paraformaldehyde, stained with 1% crystal violet, and counted using a bright-field microscope at ×100 high-power field. For each data point the number of cells in five random fields was determined.

Gel-Contraction Assay

This was conducted using 5 mL of rat tail collagen I solution (2 mg/mL in 0.1% acetic acid) mixed with 1 mL of 10 × DMEM and 1 mL of 0.1 N NaOH to neutralize the pH before adding MFs or HFs (3×10^5 cells/mL) transfected

with P311 or EV control in 3 mL of culture medium. Two milliliters of the mixed collagen gel solution was dispensed into 35-mm culture plastic plates. After incubation at 37°C for 30 minutes, polymerized gels were detached and covered with 2 mL of culture medium. Lattices were photographed after detachment on day 0 and day 2, and the magnitude of gel contraction was calculated compared with day 0.

TGF-β Rescue Experiments

Excisional wounds were generated on P311$^{-/-}$ and WT mice as described above. Twenty-four hours later, 250 ng of either recombinant (r) human TGF-β1, rTGF-β2, or rTGF-β3 (R&D Systems) dissolved in 30 μL of PBS were subcutaneously injected at the borders of the P311$^{-/-}$ wounds at four equidistant points. The WT mice received PBS. Injections were given twice a week. After 21 days, the scars were removed for HYP assays.

Statistical Analysis

The *t*-test was used for statistical comparison of two groups. All data are reported as means ± SD of the means (SEM). All experiments were repeated at least three times with reproducible results. P values <0.05 were considered significant ($*P < 0.05$, $**P < 0.01$, $***P < 0.001$).

Results

P311 Expression Is Up-Regulated in Skin Wounds and in Normal and Hypertrophic Scars

Real-time quantitative PCR (qPCR) studies demonstrated that P311 mRNA expression was increased on day 14 after wounds compared with normal skin and remained high in subsequent scars (Figure 1A). As expected, P311 mRNA was absent in the wounds and scars of P311$^{-/-}$ mice (Figure 1A). Western blot analysis showed no P311 protein expression in WT normal skin, whereas P311 was detected in healing wounds (day 14 after wound) and increased in subsequent scars (day 21 after wound) (Figure 1B). In addition, IHC showed robust P311 expression in the dermal fibroblasts of human hypertrophic scars (Figure 1C), whereas normal skin was negative (Figure 1C).

Skin Scars in P311$^{-/-}$ Mice Have Decreased TGF-β1 to -β3 Levels/Activity

Because we previously found that P311 promotes TGF-β1 to -β3 translation,[1] we determined the TGF-β1 to -β3 levels as well as SMAD2 and SMAD3 phosphorylation levels, as an indication of TGF-β1 to -β3 activity, in the scars of WT and P311$^{-/-}$ mice. ELISAs demonstrated that the scars of P311$^{-/-}$ mice had a significant decrease in the levels of TGF-β1 to -β3 (Figure 2A), and immunoblot analysis showed reduced SMAD2 and SMAD3 phosphorylation (Figure 2B).

Lack of P311 in skin scars results in decreased collagen deposition as demonstrated by HYP-incorporation assays (Figure 3A), qPCR for COL1A1 and COL3A1 (Figure 3B), immunoblotting for COL1A1 and COL3A1 (Figure 3C), and SHG imaging for detection of collagen fibers (Figure 3D) in the scars of P311$^{-/-}$ mice compared with WT controls. In addition, HYP assays demonstrated that down-regulation of P311 in the scars of WT mice by lentivirus-mediated RNA interference resulted in down-regulation of collagen production (Figure 3E), whereas its expression in scars of P311$^{-/-}$ mice lead to the opposite

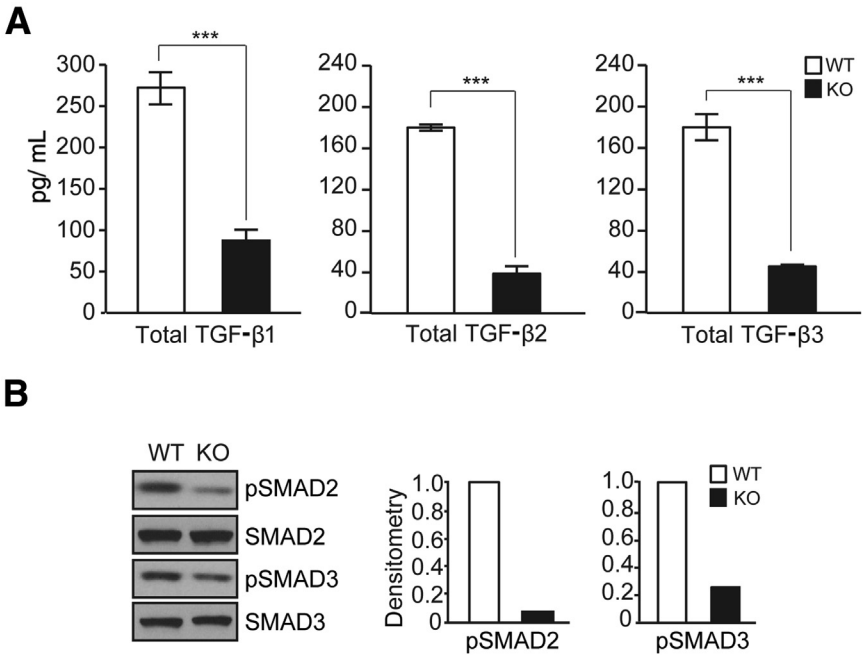

Figure 2 Skin scars in P311$^{-/-}$ mice have decreased TGF-β1 to -β3 levels/activity. **A:** ELISA assay showing total TGF-β1 to -β3 expression in WT and P311$^{-/-}$ mice scars. **B:** Representative Western blot analyses and corresponding densitometric analysis of total and pSMAD2 and pSMAD3 in WT and P311$^{-/-}$ mice scars Data are expressed as means ± SD. $n = 5$ per group (**A**); $n = 3$ per group (**B**). $***P < 0.001$. ELISA, enzyme-linked immunosorbent assay; KO, knockout; P311, neuronal protein 3.1; p, phosphorylated; TGF, transforming growth factor; WT, wild-type.

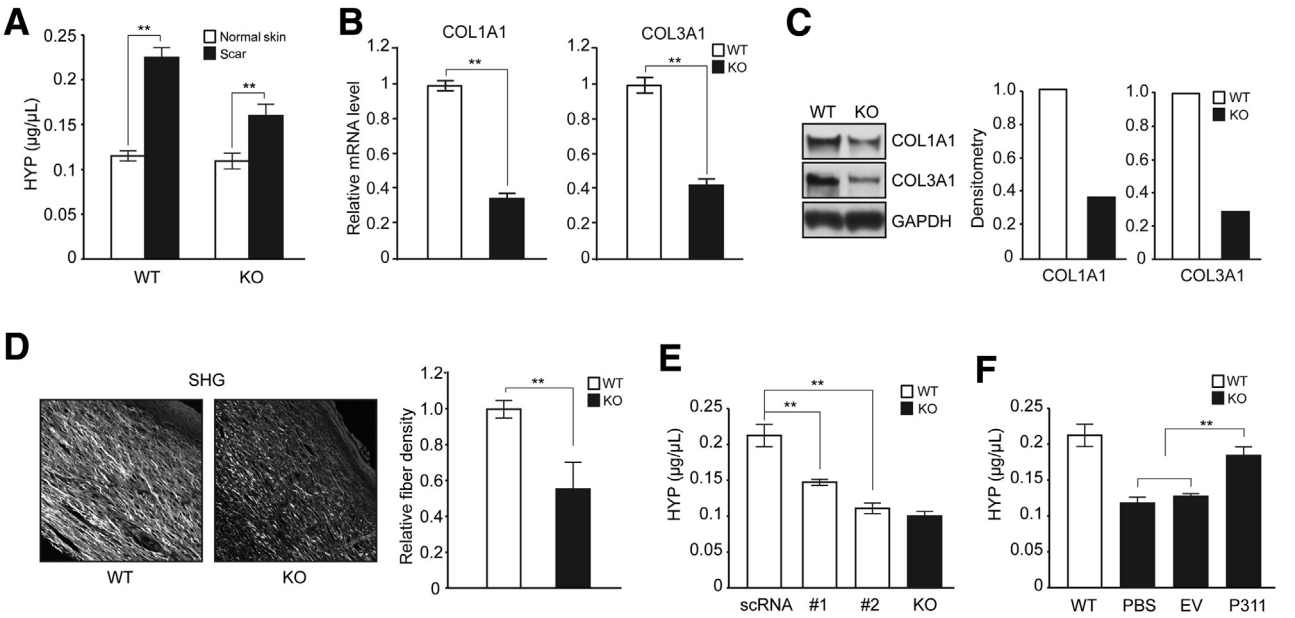

Figure 3 Lack of P311 in skin scars results in decreased collagen deposition. **A:** HYP determination assay showing HYP content in normal skin and scar tissue from WT and P311$^{-/-}$ mice. **B:** qPCR showing mRNA levels of COL1A1 and COL3A1 in WT and P311$^{-/-}$ scars. **C:** Representative Western blot analyses and corresponding densitometric analysis showing expression of COL1A1 and COL3A1 in WT and P311$^{-/-}$ scars. **D:** SHG imaging and quantitative density measurement of collagen fibers in WT and P311$^{-/-}$ scars. **E:** HYP determination assay showing HYP content in scar tissue of WT mice, with or without lentivirus-mediated knockdown of P311. **F:** HYP determination assay showing HYP content in scar tissue of WT mice, with or without lentivirus-mediated expression of P311. Data are expressed as means ± SD. $n = 3$ mice per group (**A**); $n = 3$ scars per group (**B**–**D**); $n = 4$ per group (**E** and **F**). $^{**}P < 0.01$. Original magnification, ×20 (**D**). COL1A1, collagen 1A1; COL3A1, collagen 3A1; EV, empty vector; HYP, hydroxyproline; KO, knockout; P311, neuronal protein 3.1; PBS, phosphate buffered saline; qPCR, real-time quantitative PCR; scRNA, scrambled control RNA; SHG, second-harmonic generation; WT, wild-type.

effect (Figure 3F). The scar closure time and its area and thickness did not differ between WT and P311$^{-/-}$ mice (Supplemental Figure S1).

Skin Scars in P311$^{-/-}$ Mice Have Decreased Stiffness and Tensile Strength

AFM showed similar stiffness in normal skin of WT and P31−1$^{-/-}$ mice but decreased stiffness in scars from P311$^{-/-}$ mice compared with scars from WT animals (Figure 4A). Similarly, tensile strength determination revealed decreased tensile strength in scars from P311$^{-/-}$ mice compared with scars from WT animals (Figure 4B).

P311 Stimulates TGF-β1 to -β3 Translation and Collagen Production by Dermal Fibroblasts

P311 or empty virus were transfected into MFs and HFs, which under normal conditions lack this protein (Figure 5A). qPCR results demonstrated no significant differences in TGF-β1 to -β3 mRNA levels in MFs and in TGF-β1 to -β2 mRNA levels HFs expressing P311 compared with those bearing EV control (Figure 5B). However, ELISA showed increased levels of TGF-β1 to -β3 in P311-positive MFs and increased levels of TGF-β1 to -β2 in P311-positive HFs compared with controls (Figure 5C), consistent with a P311-mediated increase in TGF-β translation. Notice that TGF-β3 was undetected in HFs (Figure 5C), despite that its message increased on P311 transfection. The P311 effect on TGF-β translation was confirmed by TGF-β translation-reporter assays, which also demonstrated the involvement of the known P311 binding partner eIF3b,[1] so that on eIF3b down-regulation, the absence of P311 suppressed TGF-β translation more dramatically than when eIF3b was present (Figure 5D). As in the scars, the P311-mediated increase in TGF-β1 to -β3 levels resulted in an increase in their activity, as indicated by increased SMAD2 and SMAD3 phosphorylation (Figure 5E). Furthermore, consistent what was observed in the scars, qPCR and immunoblot assays demonstrated

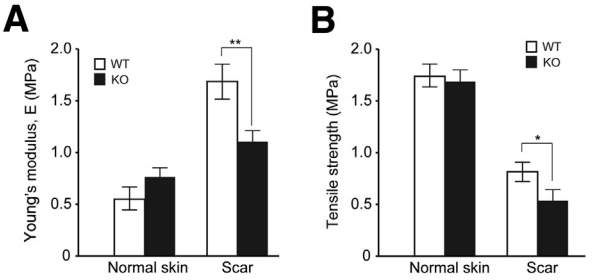

Figure 4 Skin scars in P311$^{-/-}$ mice have decreased stiffness and tensile strength. **A:** AFM stiffness characterization of normal skin and scar tissue in WT and P311$^{-/-}$ mice. **B:** Tensile strength characterization of normal skin and scar tissue in WT and P311$^{-/-}$ mice. Data are expressed as means ± SD. $n = 3$ mice per group. $^{*}P < 0.05$, $^{**}P < 0.01$. AFM, atomic-force microscopy; E, elastic modulus; KO, knockout; P311, neuronal protein 3.1; WT, wild-type.

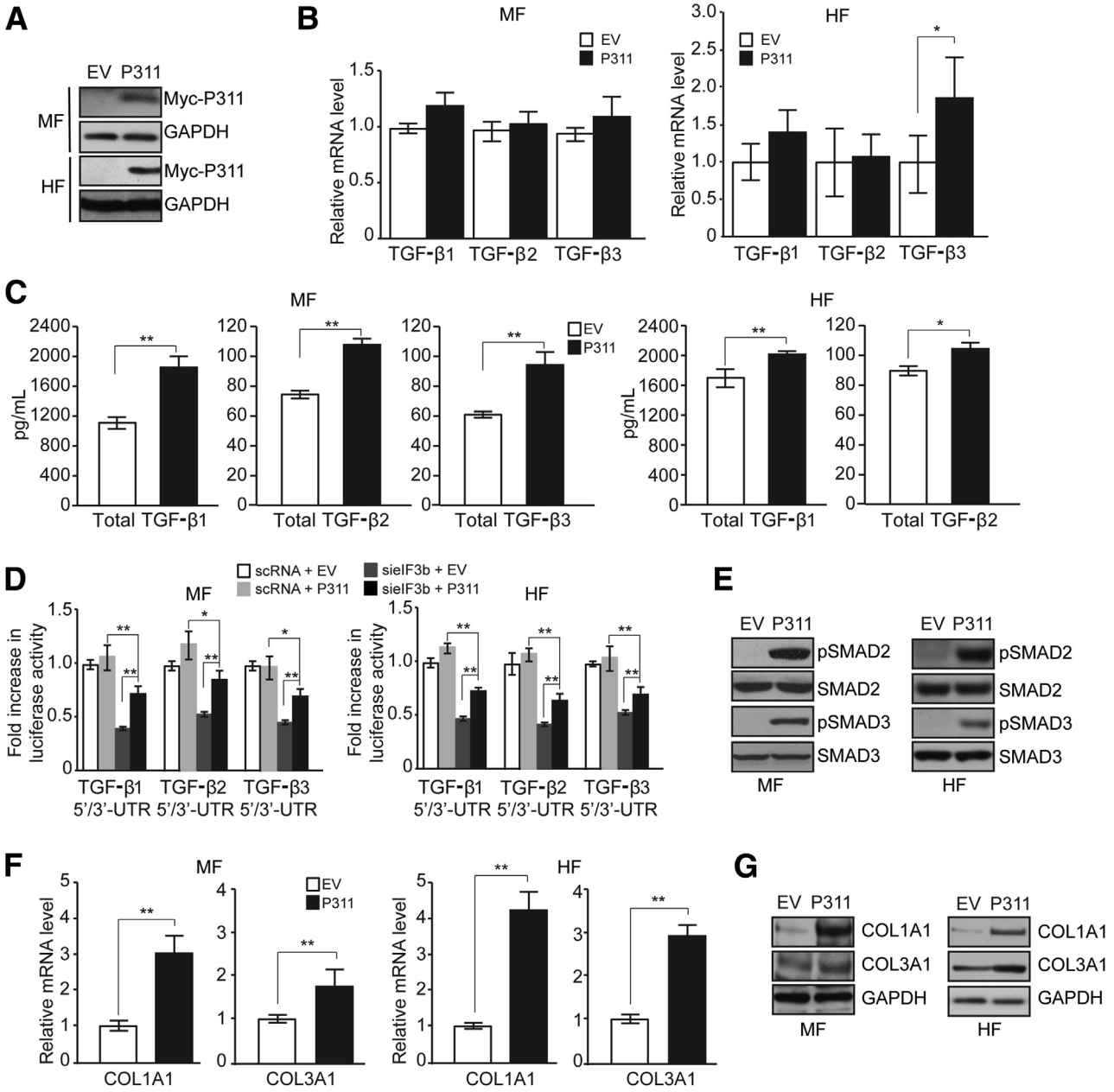

Figure 5 P311 stimulates TGF-β1 to -β3 translation and collagen production by dermal fibroblasts. **A:** Western analyses showing P311 expression in MFs and HFs transfected with EV or with a P311 plasmid construct (Myc-P311). **B:** qPCR showing levels of TGF-β1 to -β3 mRNAs in MFs and HFs transfected with EV or P311. **C:** ELISA showing levels of total TGF-βs in MFs and HFs transfected with EV or P311. **D:** Luciferase reporter assay showing 5′/3′ UTRs in MFs and HFs transfected with EV or P311 plus eIF3b siRNA or scRNA. **E:** Representative Western blot analyses showing total and active SMAD2/3 in MFs and HFs transfected with P311 or EV. **F:** qPCR showing expression of COL1A1 and COL3A1 mRNA in MFs and HFs transfected with EV or P311. **G:** Representative Western blot analyses showing expression of COL1A1 and COL3A1 in MFs and HFs transfected with EV or P311. Data are expressed as means ± SD. $n = 4$ group (**B** and **C**); $n = 3$ group (**D**–**G**), $^{*}P < 0.05$, $^{**}P < 0.01$. COL1A1, collagen 1A1; COL3A1, collagen 3A1; ELISA, enzyme-linked immunosorbent assay; EV, empty vector; GAPDH, glyceraldehyde-3-phosphate dehydrogenase; HF, human fibroblast; MF, mouse fibroblast; P311, neuronal protein 3.1; p, phosphorylated; qPCR, real-time quantitative PCR; scRNA, scrambled control RNA; sieIF3B, small interfering eukaryotic translation initiation factor 3 subunit b; TGF, transforming growth factor; UTR, untranslated region.

increased production of COL1A1 and COL3A1 in P311-positive MFs and HFs compared with their negative counterparts (Figure 5, F and G).

qPCR results demonstrated no significant differences in TGF-β1 to -β3 mRNA levels in HKs after P311 transfection compared with those bearing EV control (Supplemental Figure S2A). ELISA, however, showed increased levels of TGF-β1 to -β3 in P311-expressing HKs (Supplemental Figure S2B). Despite the increase in TGF-β1 to -β3, but consistent with the well-known lack of collagen production by keratinocytes, qPCR showed no increase in COL1A1 and COL3A1 mRNA expression on P311 transfection

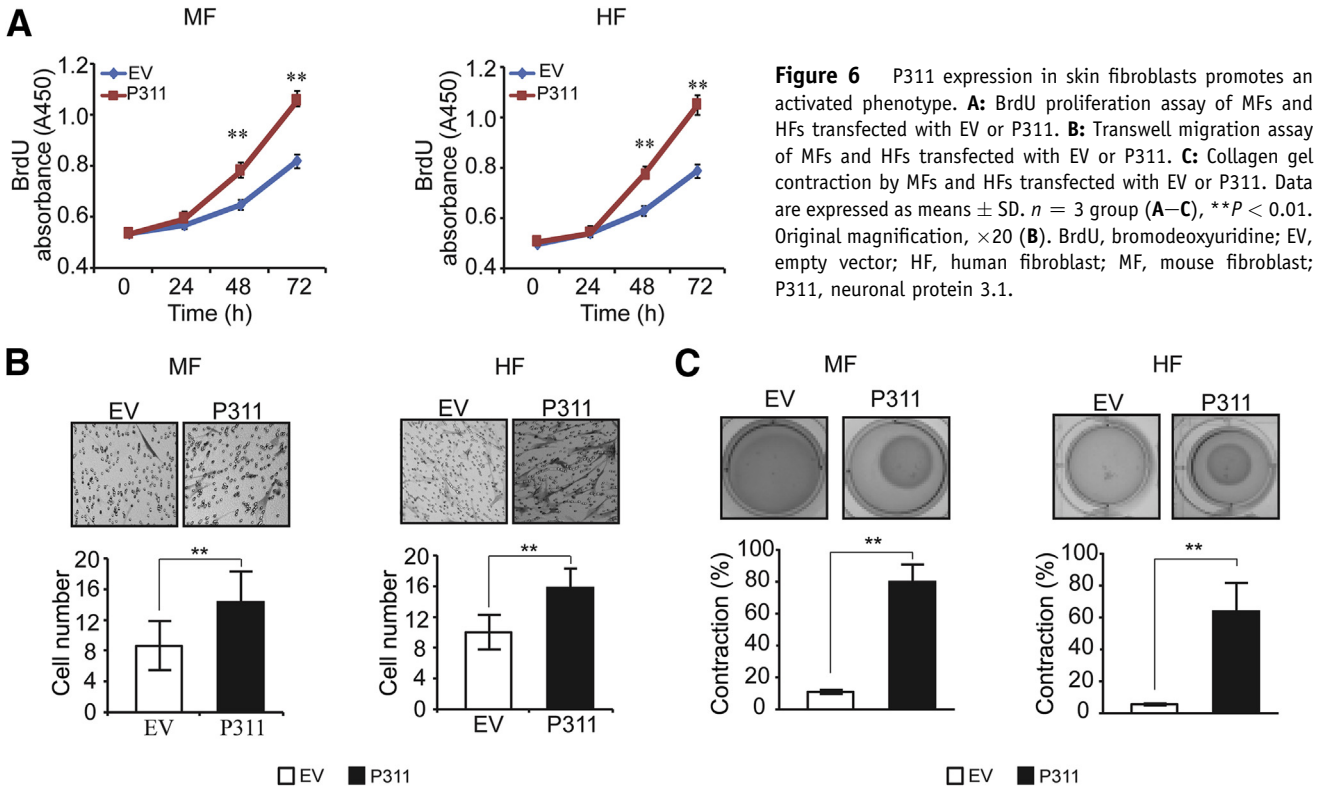

Figure 6 P311 expression in skin fibroblasts promotes an activated phenotype. **A:** BrdU proliferation assay of MFs and HFs transfected with EV or P311. **B:** Transwell migration assay of MFs and HFs transfected with EV or P311. **C:** Collagen gel contraction by MFs and HFs transfected with EV or P311. Data are expressed as means ± SD. $n = 3$ group (**A**–**C**), $^{**}P < 0.01$. Original magnification, ×20 (**B**). BrdU, bromodeoxyuridine; EV, empty vector; HF, human fibroblast; MF, mouse fibroblast; P311, neuronal protein 3.1.

(Supplemental Figure S2C), and immunoblot showed no production of COL1A1 and COL3A1 by HKs with or without P311 (Supplemental Figure S2D).

P311 Expression in Dermal Fibroblasts Promotes an Activated Phenotype

We then performed *in vitro* functional studies using MFs and HFs. These studies demonstrated that P311 increased proliferation (Figure 6A), promoted migration (Figure 6B), and increased contractility (Figure 6C) of MFs and HFs.

TGF-β1 to -β3 Rescues the Deficit in Collagen in P311$^{-/-}$ Scars

rTGF-β1, -β2, or -β3 injected at the skin wound site of P311$^{-/-}$ mice each increased HYP incorporation by scar tissue to levels similar to those observed in WT counterparts (Figure 7).

Discussion

P311 is an RNA-binding protein[1] that plays a role in cell migration, contractility, tissue regeneration, and control of systemic blood pressure.[2] Although the molecular mechanism of P311 action remained unknown for years, we recently found that P311 is an RNA-binding protein that stimulates TGF-β1 to -β3 translation *in vivo* in the vascular smooth muscle as well as in vascular smooth muscle and NIH-3T3 cells *in vitro*.[1,2]

Because TGF-β plays critical roles in fibrogenesis,[39] here we conducted studies to determine whether P311 may have a function in cutaneous scar formation. We found that P311 expression is up-regulated in excisional wounds compared with normal skin during the proliferative phase of healing, and it is further increased in expression during the remodeling phase, when the scar is formed. Confirming a previous study,[40] we also found that P311 expression remains high in hypertrophic scars. This finding suggests that P311 is likely to be involved in the process of cutaneous scarring.

Prompted by our previous work,[1,2] we determined the levels of TGF-β1 to -β3 and SMAD2 and SMAD3 phosphorylation in the scars of WT and P311$^{-/-}$ mice. As in the vascular musculature of P311$^{-/-}$ mice,[2] scars lacking P311 have a significant decrease in the level and activity of TGF-β1 to -β3.

Scars lacking P311 exhibited reduced collagen deposition with deficits in both collagen I and III. This was seen in the scars of WT mice when P311 was down-regulated, whereas P311 up-regulation in scars of P311$^{-/-}$ mice reconstituted normal collagen production. These studies established that the collagen deficiency seen in P311$^{-/-}$ scars was due to lack of P311, rather than the artifactual product of genetic manipulation.

Because scar stiffness (as opposite to elasticity) and tensile strength are largely determined by collagen content,

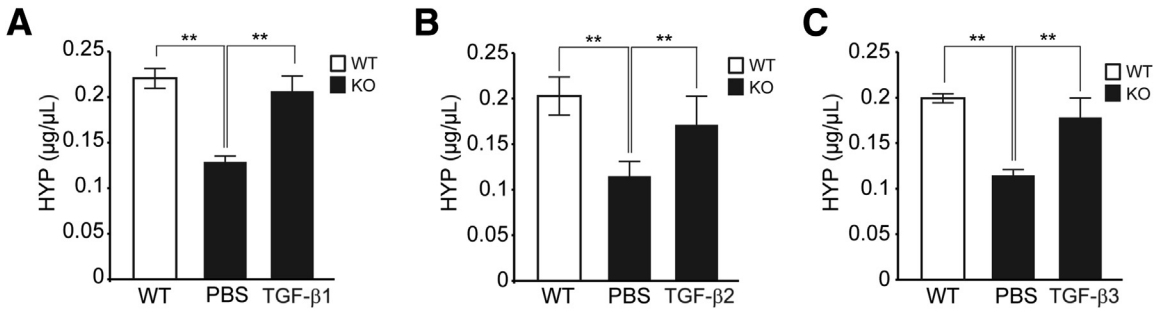

Figure 7 TGF-βs rescue the deficit in collagen in P311$^{-/-}$ scars. HYP determination assay showing HYP content in scar tissue of WT and P311$^{-/-}$ mice treated with rTGF-β1, rTGF-β2, rTGF-β3, or vehicle (PBS) alone. Data are expressed as means ± SD. $n = 4$ mice per group. $^{**}P < 0.01$. HYP, hydroxyproline; KO, knockout; P311, neuronal protein 3.1; PBS, phosphate-buffered saline; r, recombinant; TGF, transforming growth factor; WT, wild-type.

we measured these two parameters in scars from WT and P311$^{-/-}$ mice. Decreased stiffness and tensile strength were seen in scars from P311$^{-/-}$ mice compared with scars from WT animals. Reduced scar collagen formation and tensile strength have also been observed in mice lacking α11β1 integrin[41] and in diabetic rats, in which these abnormalities lead to higher incidence of dehiscence.[42] Of interest, reduced collagen deposition is not necessarily coupled with decreased tensile strength, because the opposite has been shown with poly-N-acetyl-glucosamine nanofiber treatment[43] or with the use of a selective adenosine A2AR-antagonist.[44] In both cases, reduced scar collagen content was seen with concomitantly increased tensile strength. The reasons for such differences are currently unclear.

Because fetal skin, which heals without scar formation, has significant lower levels of TGF-β1 and -β2 than adult skin, and because experimental data have demonstrated a decrease in scar size when TGF-β levels are down-regulated,[45–48] it has been proposed that a decrease in TGF-β signaling should promote scarless wound healing.[45–48] However, the scar area and thickness did not differ between WT and P311$^{-/-}$ mice in these studies. Our findings, therefore, challenge this view and point to mechanisms other than TGF-β signaling as regulators of scar size.

To understand the function of P311 at the cellular level, we conducted studies using primary cultures of MFs, HFs, and HKs. Our previous data indicated that P311 stimulates TGF-β translation in vascular smooth muscle cells as well as in NIH 3T3 cells.[2,4] Therefore, as part of the present study we determined whether P311 also has a similar effect in keratinocytes and dermal fibroblasts. To this end, we transfected P311 into MFs, HFs, and HKs, which under normal conditions lack the protein. P311 increased TGF-β1 to -β3 levels in MF and TGF-β1and -β2 in HFs without an increase in the corresponding message; findings consistent with a P311-mediated increase in TGF-β translation. Surprisingly, TGF-β3 was not detected in HFs, despite that, unlike the other TGF-βs, its message was up-regulated by P311. The effect of P311 on TGF-β translation was confirmed by translation-reporter assays, which also demonstrated the involvement of the P311 binding partner, eIF3b, in P311-mediated TGF-β1 to -β3 translation. As in scar tissue, the increase in TGF-β1 to -β3 levels was associated with an increase in their activities.

In addition, consistent what was observed in the scars, we detected increased production of COL1A1 and COL3A1 in P311-positive MFs and HFs. Although HKs responded to P311 in a similar fashion as dermal fibroblasts and increased their TGF-β levels, they did not produce COL1A1 or COL3A1, indicating their lack of involvement in the scar collagen deposition process. Significantly, the hypocollagenization and decrease in scar tensile strength observed in α11β1 integrin-null mice were also linked to defective TGF-β signaling.[41]

As part of our *in vitro* characterization effort, we performed functional studies using MFs and HFs. These showed that P311 stimulated smooth muscle actin production, increased proliferation, promoted migration, and increased contractility of both MFs and HFs, all consistent with induction of the activated state[49] and the transition to myofibroblasts.[50] In addition, P311 had an antiapoptotic effect in both cell types. All these P311-induced changes are consistent with a profibrogenic phenotype and help to understand how P311 contributes to the scar formation.

Finally, the delivery of each of the three TGF-βs to the wound site returned collagen deposition to normal levels, demonstrating that TGF-βs are the mediators whereby P311 promotes fibrosis. Our studies are supported by a recent report that showed the involvement of TGF-β1 as the mediator of P311-induced fibrosis in the kidney.[51] Here, it should be noted that TGF-β3 (as well as TGF-β1 and -β2) was able to rescue the P311$^{-/-}$ scar phenotype, standing against the widespread view that TGF-β3 serves an anti-scarring function.[15,25]

Conclusions

In summary, these studies have demonstrated that P311 is required for collagen formation and tensile strength in healing skin wounds. This, in turn, is essential to prevent scar dehiscence. Furthermore, we found that all three TGF-βs are fibrogenic and placed P311 as a stimulator of fibrosis

acting immediately upstream of TGF-β1 to -β3. Because P311 expression is up-regulated or down-regulated by hormones,[52] retinoic acid,[53] growth factors,[54] and mechanical tension,[4] and because P311 has proven to be decreased in muscular atrophy[55,56] and pulmonary emphysema,[6] it is likely that in pathologic conditions with decreased P311 expression scar formation will be affected in ways similar to those presented in this study, leading thereby to a higher risk of dehiscence.

Supplemental Data

Supplemental material for this article can be found at *http://dx.doi.org/10.1016/j.ajpath.2016.10.004*.

References

1. Yue MM, Lv K, Meredith SC, Martindale JL, Gorospe M, Schuger L: Novel RNA-binding protein P311 binds eukaryotic translation initiation factor 3 subunit b (eIF3b) to promote translation of transforming growth factor beta1-3 (TGF-beta1-3). J Biol Chem 2014, 289: 33971−33983
2. Badri KR, Yue M, Carretero OA, Aramgam SL, Cao J, Sharkady S, Kim GH, Taylor GA, Byron KL, Shuger L: Blood pressure homeostasis is maintained by a P311-TGF-beta axis. J Clin Invest 2013, 123:4502−4512
3. Studler JM, Glowinski J, Levi-Strauss M: An abundant mRNA of the embryonic brain persists at a high level in cerebellum, hippocampus and olfactory bulb during adulthood. Eur J Neurosci 1993, 5: 614−623
4. Pan D, Zhe X, Jakkaraju S, Taylor GA, Schuger L: P311 induces a TGF-beta1-independent, nonfibrogenic myofibroblast phenotype. J Clin Invest 2002, 110:1349−1358
5. Fujitani M, Yamagishi S, Che YH, Hata K, Kubo T, Ino H, Tohyama M, Yamashita T: P311 accelerates nerve regeneration of the axotomized facial nerve. J Neurochem 2004, 91:737−744
6. Zhao L, Leung JK, Yamamoto H, Goswami S, Kheradmand F, Vu TH: Identification of P311 as a potential gene regulating alveolar generation. Am J Respir Cell Mol Biol 2006, 35:48−54
7. Tan J, Peng X, Luo G, Ma B, Cao C, He W, Yuan S, Li S, Wilkins JA, Wu J: Investigating the role of P311 in the hypertrophic scar. PLoS One 2010, 5:e9995
8. Mariani L, McDonough WS, Hoelzinger DB, Beaudry C, Kaczmarek E, Coons SW, Giese A, Moghaddam M, Seiler RW, Berens ME: Identification and validation of P311 as a glioblastoma invasion gene using laser capture microdissection. Cancer Res 2001, 61:4190−4196
9. Shi J, Badri KR, Choudhury R, Schuger L: P311-induced myofibroblasts exhibit ameboid-like migration through RalA activation. Exp Cell Res 2006, 312:3432−3442
10. Taylor GA, Rodriguiz RM, Greene RI, Daniell X, Henry SC, Crooks KR, Kotloski R, Tessarollo L, Phillips LE, Wetsel WC: Behavioral characterization of P311 knockout mice. Genes Brain Behav 2008, 7:786−795
11. Sun YG, Gao YJ, Zhao ZQ, Huang B, Yin J, Taylor GA, Chen ZF: Involvement of P311 in the affective, but not in the sensory component of pain. Mol Pain 2008, 4:23
12. Sun YB, Qu X, Caruana G, Li J: The origin of renal fibroblasts/myofibroblasts and the signals that trigger fibrosis. Differentiation 2016, 92:102−107
13. Fan Z, Guan J: Antifibrotic therapies to control cardiac fibrosis. Biomater Res 2016, 20:13
14. Weiskirchen R, Tacke F: Liver fibrosis: from pathogenesis to novel therapies. Dig Dis 2016, 34:410−422
15. Lichtman MK, Otero-Vinas M, Falanga V: Transforming growth factor beta (TGF-beta) isoforms in wound healing and fibrosis. Wound Repair Regen 2016, 24:215−222
16. Meng XM, Nikolic-Paterson DJ, Lan HY: TGF-beta: the master regulator of fibrosis. Nat Rev Nephrol 2016, 12:325−338
17. Morikawa M, Derynck R, Miyazono K: TGF-beta and the TGF-beta family: context-dependent roles in cell and tissue physiology. Cold Spring Harb Perspect Biol 2016, 8:a021873
18. Biressi S, Miyabara EH, Gopinath SD, Carlig PM, Rando TA: A Wnt-TGFbeta2 axis induces a fibrogenic program in muscle stem cells from dystrophic mice. Sci Transl Med 2014, 6:267ra176
19. Echeverria C, Montorfano I, Tapia P, Riedel C, Cabello-Verrugio C, Simon F: Endotoxin-induced endothelial fibrosis is dependent on expression of transforming growth factors beta1 and beta2. Infect Immun 2014, 82:3678−3686
20. Ma B, Kang Q, Qin L, Cui L, Pei C: TGF-beta2 induces transdifferentiation and fibrosis in human lens epithelial cells via regulating gremlin and CTGF. Biochem Biophys Res Commun 2014, 447:689−695
21. Wang B, Koh P, Winbanks C, Coughlan MT, McClelland A, Watson A, Jandeleit-Dahm K, Burns WC, Thomas MC, Cooper ME, Kantharidis P: miR-200a Prevents renal fibrogenesis through repression of TGF-beta2 expression. Diabetes 2011, 60:280−287
22. Shah M, Foreman DM, Ferguson MW: Neutralisation of TGF-beta 1 and TGF-beta 2 or exogenous addition of TGF-beta 3 to cutaneous rat wounds reduces scarring. J Cell Sci 1995, 108:985−1002
23. Xu L, Xiong S, Guo R, Yang Z, Wang Q, Xiao F, Wang H, Pan X, Zhu M: Transforming growth factor beta3 attenuates the development of radiation-induced pulmonary fibrosis in mice by decreasing fibrocyte recruitment and regulating IFN-gamma/IL-4 balance. Immunol Lett 2014, 162:27−33
24. Guo X, Hutcheon AE, Zieske JD: Molecular insights on the effect of TGF-beta1/-beta3 in human corneal fibroblasts. Exp Eye Res 2016, 146:233−241
25. Profyris C, Tziotzios C, Do Vale I: Cutaneous scarring: pathophysiology, molecular mechanisms, and scar reduction therapeutics Part I. The molecular basis of scar formation. J Am Acad Dermatol 2012, 66:1−10. quiz 11−12
26. Papakonstantinou E, Aletras AJ, Roth M, Tamm M, Karakiulakis G: Hypoxia modulates the effects of transforming growth factor-beta isoforms on matrix-formation by primary human lung fibroblasts. Cytokine 2003, 24:25−35
27. Lu L, Saulis AS, Liu WR, Roy NK, Chao JD, Ledbetter S, Mustoe TA: The temporal effects of anti-TGF-beta1, 2, and 3 monoclonal antibody on wound healing and hypertrophic scar formation. J Am Coll Surg 2005, 201:391−397
28. Coker RK, Laurent GJ, Shahzeidi S, Lympany PA, du Bois RM, Jeffery PK, McAnulty RJ: Transforming growth factors-beta 1, -beta 2, and -beta 3 stimulate fibroblast procollagen production in vitro but are differentially expressed during bleomycin-induced lung fibrosis. Am J Pathol 1997, 150:981−991
29. Andreola F, Calvisi DF, Elizondo G, Jakowlew SB, Mariano J, Gonzalez FJ, De Luca LM: Reversal of liver fibrosis in aryl hydrocarbon receptor null mice by dietary vitamin A depletion. Hepatology 2004, 39:157−166
30. Akhurst RJ, Hata A: Targeting the TGFbeta signalling pathway in disease. Nat Rev Drug Discov 2012, 11:790−811
31. Block L, Gosain A, King TW: Emerging therapies for scar prevention. Adv Wound Care (New Rochelle) 2015, 4:607−614
32. Varani J, Schuger L, Dame MK, Leonard C, Fligiel SE, Kang S, Fisher GJ, Voorhees JJ: Reduced fibroblast interaction with intact collagen as a mechanism for depressed collagen synthesis in photodamaged skin. J Invest Dermatol 2004, 122:1471−1479
33. Liskova J, Babchenko O, Varga M, Kromka A, Hadraba D, Svindrych Z, Burdikova Z, Bacakova L: Osteogenic cell

differentiation on H-terminated and O-terminated nanocrystalline diamond films. Int J Nanomedicine 2015, 10:869−884
34. Kolar K: Colorimetric determination of hydroxyproline as measure of collagen content in meat and meat products: NMKL collaborative study. J Assoc Off Anal Chem 1990, 73:54−57
35. Hutter JL, Bechoefer J: Calibration of Atomic-Force Microscope Tips. Rev Sci Instrum 1993, 64:1868−1873
36. Sneddon IN: The relation between load and penetration in the axisymmetric boussinesq problem for a punch of arbitrary profile. Int J Eng Sci 1965, 3:47−57
37. Wang X, Bleher R, Brown ME, Garcia JG, Dudek SM, Shekhawat GS, Dravid VP: Nano-biomechanical study of spatio-temporal cytoskeleton rearrangements that determine subcellular mechanical properties and endothelial permeability. Sci Rep 2015, 5:11097
38. Thomay AA, Daley JM, Sabo E, Worth PJ, Shelton LJ, Harty MW, Reichner JS, Albina JE: Disruption of interleukin-1 signaling improves the quality of wound healing. Am J Pathol 2009, 174:2129−2136
39. Meng XM, Chung AC, Lan HY: Role of the TGF-beta/BMP-7/Smad pathways in renal diseases. Clin Sci (Lond) 2013, 124:243−254
40. Wu J, Ma B, Yi S, Wang Z, He W, Luo G, Chen X, Wang X, Chen A, Barisoni D: Gene expression of early hypertrophic scar tissue screened by means of cDNA microarrays. J Trauma 2004, 57:1276−1286
41. Schulz JN, Zeltz C, Sørensen IW, Barczyk M, Carracedo S, Hallinger R, Niehoff A, Eckes B, Gullberg D: Reduced granulation tissue and wound strength in the absence of alpha11beta1 integrin. J Invest Dermatol 2015, 135:1435−1444
42. Minossi JG, Lima Fde O, Caramori CA, Hasimoto CN, Ortolan EV, Rodrigues PA, Spadella CT: Alloxan diabetes alters the tensile strength, morphological and morphometric parameters of abdominal wall healing in rats. Acta Cir Bras 2014, 29:118−124
43. Lindner HB, Felmly LM, Demcheva M, Seth A, Norris R, Bradshaw AD, Vournakis J, Muise-Helmericks RC: pGlcNAc nanofiber treatment of cutaneous wounds stimulate increased tensile strength and reduced scarring via activation of Akt1. PLoS One 2015, 10:e0127876
44. Perez-Aso M, Chiriboga L, Cronstein BN: Pharmacological blockade of adenosine A2A receptors diminishes scarring. FASEB J 2012, 26: 4254−4263
45. Walraven M, Gouverneur M, Middelkoop E, Beelen RH, Ulrich MM: Altered TGF-beta signaling in fetal fibroblasts: what is known about the underlying mechanisms? Wound Repair Regen 2014, 22:3−13
46. Zhao F, Wang Z, Lang H, Liu X, Zhang D, Wang X, Zhang T, Wang R, Shi P, Pang X: Dynamic expression of novel MiRNA candidates and MiRNA-34 family members in early- to mid-gestational fetal keratinocytes contributes to scarless wound healing by targeting the TGF-beta pathway. PLoS One 2015, 10:e0126087
47. Tarzemany R, Jiang G, Larjava H, Häkkinen L: Expression and function of connexin 43 in human gingival wound healing and fibroblasts. PLoS One 2015, 10:e0115524
48. Li H, Duann P, Lin PH, Zhao L, Fan Z, Tan T, Zhou X, Sun M, Fu M, Orange M, Sermersheim M, Ma H, He D, Steinberg SM, Higgins R, Zhu H, John E, Zeng C, Guan J, Ma J: Modulation of wound healing and scar formation by MG53 protein-mediated cell membrane repair. J Biol Chem 2015, 290:24592−24603
49. Shaw TJ, Martin P: Wound repair: a showcase for cell plasticity and migration. Curr Opin Cell Biol 2016, 42:29−37
50. Hinz B: Myofibroblasts. Exp Eye Res 2016, 142:56−70
51. Yao Z, Yang S, He W, Li L, Xu R, Zhang X, Li H, Zhan R, Sun W, Tan J, Zhou J, Luo G, Wu J: P311 promotes renal fibrosis via TGFbeta1/Smad signaling. Sci Rep 2015, 5:17032
52. Baran N, Kelly PA, Binart N: Characterization of a prolactin-regulated gene in reproductive tissues using the prolactin receptor knockout mouse model. Biol Reprod 2002, 66:1210−1218
53. Leung JK, Cases S, Vu TH: P311 functions in an alternative pathway of lipid accumulation that is induced by retinoic acid. J Cell Sci 2008, 121:2751−2758
54. Taylor GA, Hudson E, Resau JH, Vande Woude GF: Regulation of P311 expression by Met-hepatocyte growth factor/scatter factor and the ubiquitin/proteasome system. J Biol Chem 2000, 275:4215−4219
55. Lecker SH, Jagoe RT, Gilbert A, Gomes M, Baracos V, Bailey J, Price SR, Mitch WE, Goldberg AL: Multiple types of skeletal muscle atrophy involve a common program of changes in gene expression. FASEB J 2004, 18:39−51
56. Ooi PT, da Costa N, Edgar J, Chang KC: Porcine congenital splayleg is characterised by muscle fibre atrophy associated with relative rise in MAFbx and fall in P311 expression. BMC Vet Res 2006, 2:23